Oligomerization of cytochrome *c*, myoglobin, and related heme proteins by 3D domain swapping

Shun Hirota*

Division of Materials Science, Graduate School of Science and Technology, Nara Institute of Science and Technology, 8916-5 Takayama, Ikoma, Nara, 630-0192, Japan

*Corresponding author.

E-mail address: hirota@ms.naist.jp (S. Hirota).

Abstract

Oligomerization of heme proteins is useful for construction of new materials with cooperative and systematic functions; thus, diverse methods have been applied for construction of artificial heme protein oligomers. Three-dimensional (3D) domain swapping is a protein oligomerization phenomenon that exchanges the same domain or secondary structural element between molecules. 3D domain swapping was first reported in 1994; since then many proteins have been reported to domain swap. Our research group has been showing that various heme proteins domain swap. We also found that domain swapping of heme proteins occurs at the early stage of protein folding, and utilized it to construct various heme protein assemblies, including nanorings, cages, hetero dimers with different active sites, and a ligand-binding reversible monomer–polymer system. In this review, the basics and applications of domain swapping of heme proteins are summarized.

Keywords: 3D domain swapping; designer protein; heme protein; protein oligomer; protein polymer; supramolecular hemoprotein

1. Introduction

Supramolecular chemistry is developing remarkably; for example, large metal–organic frameworks with molecular encapsulating properties are expected to be useful for applications such as gas storage, catalysis, and sensing [1-5]. Heme proteins are responsible for various biological activities, including electron transfer, oxygen transport/storage, substrate oxidation, signal transduction, etc. [6,7]. Multi-heme proteins that contain more than one heme unit in a single protein macromolecule exist in nature, where they perform a wide variety of tasks: redox communication, long-range electron transfer, and storage of reducing/oxidizing equivalents [8-10].

Many artificial heme protein oligomers have been constructed for future materials by diverse methods. For example, Tezcan and coworkers used metal coordination to construct heme protein assemblies of cytochrome (cyt) *cb*$_{562}$ [11,12] , in which the heme was immobilized on the 4-helix bundle protein moiety by introducing two cysteine (Cys) residues. By introducing histidine (His) to the third helix from the N-terminus of cyt *cb*$_{562}$, a metal binding site was composed of the introduced His residues of different molecules, resulting in the formation of tetramers, dimers, and trimers by coordination of Zn^{2+}, Cu^{2+}, and Ni^{2+}, respectively [11]. Additionally, one-dimensional helical nanotubes and two- or three-dimensional protein crystalline arrays were obtained at different pH and Zn^{2+} concentrations when two Zn^{2+} binding sites with different affinities were introduced to the protein surface of cyt *cb*$_{562}$ [12]. Hayashi, Oohora, and coworkers have constructed protein oligomeric assemblies by chemically modifying a heme on the protein surface of cyt *b*$_{562}$ through a genetically-introduced Cys and initiating successive interprotein heme–heme pocket interactions [13]. Later, they succeeded in obtaining cyt *b*$_{562}$ oligomers with a periodic structure by controlling the hydrogen bonding and/or electrostatic interactions at the protein interface [14]. A giant amphiphilic assembly

which formed vesicular structures in solution was obtained by coupling a polystyrene chain to the propionate side chain of the heme of horseradish peroxidase with a hydrophilic bis(aminoethoxy)ethane spacer [15]. Furthermore, a fusion protein comprising cyt *b* and a tandem repeat of the Src homology 3 (SH3) domain has been demonstrated to construct a fibrous structure [16], whereas myoglobin and cyt *c* have been shown to form amyloid fibrils [17,18].

Proteins can oligomerize by exchanging the same domain or secondary structural element between molecules; the phenomenon termed '3D domain swapping' (herein, domain swapping) [19-22]. The word '3D' is used to clarify that the protein domains are not exchanged genetically but three-dimensionally. Crestfield and co-workers introduced the concept of domain swapping in 1962 for the dimer of bovine pancreatic ribonuclease (RNase) A exchanging the N-terminal domains [23], and Eisenberg and co-workers first used the term 'domain swapping' for diphtheria toxin in 1994 by comparing the three dimensional structures of the monomer and dimer [24]. Since then, many proteins have been shown to domain swap according to their X-ray crystal structures. Among them, RNase A oligomerizes exchanging the N-terminal or C-terminal region [20]. A flagellar motor protein FliG exists predominantly as a monomer in solution, but self-assembles into domain-swapped polymers in flagellar motors by interacting with a structural template [25]. Attempts to control domain swapping and protein function have also been made. For example, Woolley and co-workers designed a light-induced domain swapping switch [26]. Loh and coworkers regulated a protein function utilizing a fusion protein of a recognition protein that binds a triggering molecule and a target protein that undergoes domain swapping in response to binding of the triggering ligand [27]. Arai and co-workers constructed a stable domain-swapped four-helix bundle dimer [28], and used it to construct self-assembling artificial nanoarchitectures [29]. Currently, domain swapping is recognized as a

common phenomenon in the protein science field; however, its biological role and mechanism are still under debate.

Although domain swapping has been observed in a variety of proteins, there had been only a limited number of reports on domain-swapped heme proteins until recently [30-34]. Knowledge on domain swapping in heme proteins will help us understand the fundamental properties of domain swapping. Additionally, domain swapping of heme proteins is a useful method to construct accumulated heme cofactors for new biomaterials with cooperative and systematic functions [35,36]. Thus, our group has focused on intentionally constructing domain-swapped oligomers of heme proteins and investigating their properties; examples of domain-swapped heme proteins from our group and others are listed in Table 1. The structural aspect, property, mechanism, and utilization of domain swapping in heme proteins are summarized in this review.

2. Domain swapping of *c*-type cytochromes and myoglobin

2.1 Polymerization and activity change in cytochrome *c*

Cyt *c* is a water-soluble heme protein that transfers electrons in the respiratory chain of mitochondria, as well as playing a role in apoptosis [37,38]. Cyt *c* contains three long α-helices, and its heme is attached to the polypeptide at the N-terminal α-helix. His and methionine (Met) of the polypeptide are coordinated to the heme iron in the natural state of cyt *c* [39,40]. Cyt *c* has long been used as a model protein for studies on the structure–function relationship and protein folding of proteins. While cyt *c* was reported to polymerize more than a half-century ago [41], the polymerization mechanism remained unknown until our study. We have prepared and isolated various sizes of oligomers of horse cyt *c* by treating it with ethanol, subsequently freeze-drying the solution, and redissolving the protein residue. Cyt *c* dimers and trimers were

purified from the mixture of oligomers, and the dimer and trimer crystal structures were analyzed. The α-helix in the C-terminal region was found to intermolecularly exchange between molecules in the dimer (PDB ID: 3NBS) and trimer (PDB ID: 3NBT). The structures of the C-terminal region were similar between the monomer and the protomers of the dimer and trimer, as well as the rest of the protein excluding the hinge loop. Considering these results, it was elucidated that cyt *c* polymerization occurs by successive domain swapping (runaway domain swapping; propagated domain swapping) (Figure 1) [42]. Up to now, protein polymerization by successive domain swapping has been indicated for several proteins, including RNase A [43], serpin [44], cystatin C [45], T7 endonuclease I [46], β_2-microglobulin [47], and γD-crystallin [48].

In the cyt *c* oligomers, heme-coordinating Met80 disassociated from the heme iron, and external ligands, such as the cyanide ion, were able to bind to the heme iron (Figure 1) [49]. The peroxidase activity (oxidation of substrate with hydrogen peroxide) of the dimer was increased compared to that of the monomer [50], owing to the dissociation of Met80 from the heme iron. Yeast iso-1-cyt *c* has also been shown to domain swap the C-terminal α-helix, and detergents bound into a cavity of the yeast cyt *c* dimer when the Met80 ligation was lost [51]. Interaction of positively charged cyt *c* with negatively charged cardiolipin (CL) in mitochondria plays a crucial role in triggering apoptosis by mediating release of cyt *c* to the cytosol, where the peroxidase activity of cyt *c* is thought to play an important role [52]. CL is oxidized by the peroxidase reaction of the cyt *c*–CL complex [53], and the inner membrane-bound cyt *c* is released to the intermembrane space by alterations in the membrane structure by the CL oxidation [54]. It is noteworthy that the peroxidase activity of cyt *c* increases by domain swapping, which may affect the apoptotic activity.

The enthalpy changes (ΔH) during the dissociations of dimer, trimer, and tetramer were

negative, indicating that dissociations of oligomers to monomers are exothermic processes. According to differential scanning calorimetry measurements, ΔH of the dimer-to-monomer, trimer-to-monomer, and tetramer-to-monomer dissociations were –40, –60, and –79 kcal/mol, respectively, revealing that ΔH is decreased by ~20 kcal/mol by elongation of one monomer unit [42]. The ΔH of Met coordination to the heme in cyt *c* has been estimated to be –18 kcal/mol [55]; thus, the Met dissociation from the heme iron contributed largely to the ΔH of –20 kcal/mol for oligomer dissociation. According to theoretical calculations [56], the domain-swapped cyt *c* dimer was determined to be slightly less stable than the monomer; the total free energy difference was 25 kcal/mol. The conformational change and translational/rotational entropy change destabilized the domain-swapped dimer, whereas the hydration and vibrational entropy stabilized it. The Met80 coordination to the heme iron in cyt *c* contributed to the stabilization of the monomer (ΔH = 16 kcal/mol); however, no large difference was observed between the dimer-to-monomer dissociation temperatures of wild-type (WT) and M80A cyt *c* (61.0 °C) [57]. The activation enthalpy values were similar and relatively large for the dissociation of both WT and M80A cyt *c* dimers (WT, 120±10 kcal/mol; M80A, 110±10 kcal/mol). Similar large enthalpy values were obtained for the dissociation of the *Hydrogenobacter thermophilus* (HT) domain-swapped cyt c_{552} dimer to monomers (see text below) [58]. A large activation heat capacity change was observed for dissociation of the yeast cyt *c* dimer, supporting the large structural rearrangement in the domain-swapped dimer dissociation [51]. These results revealed that the domain-swapped cyt *c* dimers suffered large structural changes upon dissociation to monomers independent of the Met80–heme iron bond and that the cyt *c* domain swapping occurs regardless of the Met80 coordination, whereas the monomer is stabilized by the Met80 coordination.

2.2 Domain swapping of other *c*-type cytochromes

Pseudomonas aeruginosa (PA) cyt c_{551} and HT cyt c_{552} exhibit similar tertiary structures (three long α-helices) as cyt *c* and belong to the *c*-type cyt protein family, although PA cyt c_{551} and HT cyt c_{552} are negatively and positively charged, respectively [59,60]. PA cyt c_{551} and HT cyt c_{552} both formed domain-swapped dimers by treatment with ethanol [58,61]. However, instead of the C-terminal α-helix, the N-terminal region containing the N-terminal α-helix and heme was exchanged between protomers in the PA cyt c_{551} dimer (PDB ID: 3X39; Figure 2A) and HT cyt c_{552} dimer (PDB ID: 3VYM; Figure 2B), where the structures of the N-terminal regions—as well as the rest of the proteins except for the hinge loops—were similar between the monomer and corresponding dimer. By inserting three Gly residues into the hinge loop of HT cyt c_{552} (insG3), two domain-swapped dimers (major and minor) were obtained [62]. The N-terminal region was exchanged in the major dimer of HT cyt c_{552} insG3 mutant (PDB ID: 5AUR; Figure 2C), whereas the C-terminal helix was exchanged in the minor dimer (PDB ID: 5AUS; Figure 2D) [62], demonstrating that *c*-types cyt can undergo both N-terminal and C-terminal domain swapping. In fact, similar dual domain swapping has been reported for RNase A [63-65]. A relatively strong hydrogen bonding network is formed at the loop containing Met that is coordinated to the heme iron in PA cyt c_{551} and HT cyt c_{552}; thus, the C-terminal α-helix following this loop may not dissociate from the rest of the protein during domain swapping, resulting in exchanging majorly the N-terminal region [58]. According to these results, domain swapping may occur at various protein sites, but the swapping region is governed by the stability and/or strength of the interaction between the swapping region and the rest of the protein.

The amount of higher order oligomers was significantly smaller for PA cyt c_{551} and HT cyt c_{552} compared to that for horse cyt *c*. It has been reported that the monomer–dimer equilibrium

in domain swapping is affected by the length and property of the hinge loop [20,66,67]. The hinge loops of domain swapping for PA cyt c_{551} and HT cyt c_{552} were composed of only 3 residues, apparently inducing the steric hindrance between the protomers during domain swapping and inhibiting formation of higher order oligomers. By elongating the hinge loop of the HT cyt c_{552} major dimer and decreasing the steric hindrance between protomers, the amount of higher order domain-swapped oligomers increased for the cyt c_{552} insG3 mutant compared to that for WT cyt c_{552} [62], supporting the hypothesis that the steric hindrance between the protomers in the N-terminal domain-swapped oligomers inhibits the formation of higher order oligomers. Interestingly, the transmission electron microscope image of the oligomers of cyt c_{552} insG3/W57K mutant exhibited well-separated protein ring structures at 7–10 nm in diameter [62]. These results demonstrate that hinge loop modification affects the size and morphology of the domain-swapped oligomers, facilitating its application in multi-heme oligomer design.

Met61 and Met59 coordinated to the heme in the domain-swapped dimers of PA cyt c_{551} and HT cyt c_{552}, respectively, but the Met residues originated from the other protomer to which the heme belonged [58,61]. The Fe–His and Fe–Met distances of the domain-swapped dimer did not differ significantly from those of the corresponding monomers in PA cyt c_{551} and HT cyt c_{552}. For example, in the insG3 cyt c_{552} major and minor dimers, the Fe–His14 distances were 2.04−2.07 Å and 2.04−2.05 Å, respectively, and the Fe−Met62 distances were 2.25−2.39 Å and 2.34−2.35 Å, respectively (major dimer PDB ID: 5AUR; minor dimer PDB ID: 5AUS) [62]. These distances were similar to the corresponding distances in the WT cyt c_{552} monomer (Fe−His14, 2.05−2.09 Å; Fe−Met59, 2.33−2.40 Å) (PDB ID: 1YNR). The midpoint redox potential (E_m) of the PA cyt c_{551} dimer was obtained as 242 mV (vs NHE), which was lower than that of the PA cyt c_{551} monomer (274 mV) [61]. E_m of the HT cyt c_{552} dimer also shifted to

a slightly lower potential at 213 mV (vs NHE) compared to that of the monomer (240 mV) [58]. However, the PA cyt c_{551} and HT cyt c_{552} dimers exhibited relatively high redox potentials, which were characteristic for *c*-type cyts, although the heme-coordinating Met residues in the dimers originated from the other protomer to which the heme belonged. It is noteworthy that the original redox potential of the heme site was maintained in the PA cyt c_{551} and HT cyt c_{552} dimers, although the heme active sites were constructed with two protomers.

Cyt c_{555} from hyperthermophilic bacterium *Aquifex aeolicus* (AA) is a hyperstable *c*-type cyt that possesses a unique extra long 3_{10}-α-3_{10} helix containing the heme-coordinating Met61 [68]. AA cyt c_{555} formed dimers by swapping the region containing the 3_{10}-α-3_{10} and C-terminal helices (PDB ID: 3X15; Figure 2E), where the overall protein structure of the dimer corresponded well to that of the monomer, except for the hinge region (Val53–Lys57) [69]. Met61 in the extra 3_{10}-α-3_{10} helix was also coordinated to the heme iron in the dimer as in the monomer, but it originated from the other protomer to which the heme belonged, similar to other domain-swapped bacterial *c*-type cyts [58,61,62]. The AA cyt c_{555} dimer dissociated to monomers at 92°C, and the secondary structures of the dimer were maintained at pH 2.2–11.0. The dimer maintained the thermostable and pH-stable properties of the monomer, apparently owing to the conservation of the secondary structures by domain swapping. Interestingly, CN^- and CO bound to the heme iron of the AA cyt c_{555} dimer in the ferric and ferrous states, respectively, in solution [69], although Met61 was coordinated to the heme iron in the crystal structure of the oxidized dimer, and these ligands did not bind to the monomer under the same conditions. The hinge region was close to Met61 in the dimer, and the flexibility of the hinge loop may have allowed these ligands to bind to the heme iron in the AA cyt c_{555} dimer. This is another example of converting a six-coordinate heme protein into a ligand-binding protein by domain swapping, in addition to cyt *c* domain swapping.

It is noteworthy that horse cyt *c* and AA cyt c_{555} swapped the C-terminal region, and the active site structures and protein properties changed by domain swapping, whereas PA cyt c_{551} and HT cyt c_{552} mainly swapped the N-terminal region, and the active site structures and protein properties did not change significantly, although all of these proteins belong to the same *c*-type cyt protein family with similar tertiary structures. The hinge loops of domain swapping for horse cyt *c* and AA cyt c_{555} were located relatively close to the active site heme, and external ligands bound to the heme irons of domain-swapped horse cyt *c* and AA cyt c_{555} dimers but not (or weakly) to their monomers [42,49,69]. On the other hand, the hinge loops for PA cyt c_{551} and HT cyt c_{552} were located relatively far from the heme, and their redox potentials did not change significantly by domain swapping [58,61]. Additionally, the hinge loops for cyt cb_{562} and AV cyt *c*′ were located relatively far from the heme, and both proteins exhibited similar properties before and after domain swapping (see text below). In this way, the property of a hemoprotein may change by domain swapping when the hinge loop is located close to the active site, whereas the property tends not to change significantly by domain swapping when the hinge loop is located far from it.

2.3 Domain swapping of myoglobin

Myoglobin (Mb) consists of 8 α-helices (A–H helix) with its heme located in the hydrophobic space between the E and F helices. When horse Mb was treated with ethanol, a dimer was obtained, but higher order oligomers were obtained in very low yields. In the Mb dimer, the E and F helices and the EF loop formed a long α helix, resulting in a domain-swapped structure (PDB ID: 3VM9; Figure 2F). Considering the domain-swapped structure, it is likely that dimers were mainly obtained owing to the hinge loop converting to a part of the long α helix in the domain-swapped dimer. Similar to *c*-type cyts, the overall protein and active site

structures of the dimer were similar to those of the monomer, except for the hinge region [70]. Although the dimer active site was formed from two Mb protomers with the proximal and distal sites of the heme originating from different protomers, the dimer exhibited high O_2 binding capacity, similar to monomeric Mb. The protein environment around the bound CO and the protein relaxation character were also similar between the CO-bound Mb monomer and dimer [71]. However, the CO binding rate constant of the Mb dimer ($(1.01 \pm 0.03) \times 10^6$ $M^{-1}s^{-1}$ at 20°C) was about twice as large as that of the monomer ($(0.52 \pm 0.02) \times 10^6$ $M^{-1}s^{-1}$ at 20°C), presumably due to the expansion of the channel between the Xe3 cavity [72] and the solvent by the dimerization.

As mentioned above, domain swapping caused horse cyt *c* to polymerize and its function changed. Mainly dimers were obtained by domain swapping of Mb, and the O_2 binding property remained unchanged but the CO binding property changed by the domain swapping. The variety in the effects of domain swapping on the function suggests the possibility of creating various types of heme protein oligomers by domain swapping. Design of a domain-swapped Mb dimer with different active sites utilizing amino acid mutation is discussed below in Section 3-1.

3. In vitro and in vivo domain swapping

3-1. Domain swapping during protein folding

The domain swapping mechanism of heme proteins is discussed in this section. The formation of horse cyt *c* domain-swapped oligomers was triggered by the Met dissociation from the heme iron by treatment with ethanol [73], although cyt *c* domain swapping occurs regardless of the Met80 coordination [57]. Ethanol decreased both the activation enthalpy and activation entropy for the dissociation of the domain-swapped dimer of HT cyt c_{552} to monomers from 140 ± 9 to 110 ± 5 kcal/mol and 310 ± 30 to 270 ± 20 cal/(mol·K), respectively [58], supporting

the hypothesis that ethanol affects domain swapping.

When cyt *c* was refolded from the guanidinium ion-denatured state, a similar domain-swapped dimer was obtained as that obtained by treatment with ethanol, and the amount of the oligomers increased when the concentration of cyt *c* for refolding was increased [74]. In the early stage of cyt *c* folding, the N-terminal and C-terminal regions form α-helices, and the two α-helices interact hydrophobically [75,76]. For the mutant in which a hydrophobic amino acid of the N-terminal α-helix was replace with glycine and the mutant in which that of the C-terminal α-helix was replaced, both mutants formed almost no oligomer when folding independently. However, when the two mutants were folded together, heterodimers of the mutants were obtained. These results indicated that domain-swapped oligomers of cyt *c* are formed when the N-terminal and C-terminal α-helices interact intermolecularly by hydrophobic interactions at the early stage of folding, whereas monomers are formed when the two α-helices interact intramolecularly (Figure 3) [74]. For domain swapping of cyt *c* during folding, the intermolecular interaction for oligomer formation of cyt *c* compared to the intramolecular interaction for monomer formation increased at low temperatures [74]. It has also been reported that RNase A domain swaps during refolding from the urea- or guanidinium ion-denatured state [77]. Thus, domain swapping during folding may be a common mechanism among different proteins.

Domain-swapped horse cyt *c* dimers, in which the C-terminal *α*-helix was exchanged between protomers, were obtained also by refolding from the molten globule state [78], where the amount of cyt *c* oligomer depended on the nature of the anion (chaotropic or kosmotropic) in the solution; more oligomers formed for chaotropic anions. About 11% of cyt *c* were obtained as oligomers by refolding from the molten globule state containing 125 mM ClO_4^-. According to small angle X-ray scattering measurements, approximately 25% of the cyt *c* molecules were

dimerized in the molten globule state containing the same amount of ClO_4^- (125 mM) [78]. These results indicated that a certain amount of molten globule state oligomers of cyt *c* converts to domain-swapped oligomers during refolding, and that the intermolecular interactions necessary for domain swapping are present in the molten globule state.

The domain-swapped dimer of apoMb was detected in the simulations of the simultaneous folding of two monomers, where the dimer exhibited a similar structure to that obtained from X-ray structure analysis [79]. The separation between the monomer folding and domain swapping in the simulation folding pathway of apoMb occurred at the early stage of folding, similar to the folding experiments of cyt *c* [74]. These results indicate that domain swapping is determined at the early stage of folding for various proteins.

3-2. Domain swapping during protein expression

Domain-swapped oligomers of HT cyt c_{552} were formed in *Escherichia coli* (*E. coli*) which expressed cyt c_{552}, and the region containing the N-terminal α-helix and heme was exchanged between protomers in the purified dimer [80]. The amount of cyt c_{552} oligomers increased in *E. coli* as the cyt c_{552} concentration was increased during culture, whereas it decreased by decreasing the protein stability with amino acid mutation, indicating that cyt c_{552} domain swapping decreases in cells when the protein stability decreases. Additionally, apo cyt c_{552} was detected in the cyt c_{552} oligomers formed in *E. coli*, but not in those of the destabilized A5F/M11V/Y32F/Y41E/I76V mutant. The cyt c_{552} oligomer containing its apo protein apparently formed at the periplasm, since the apo protein did not contain the signal peptide according to mass measurements. These results showed that domain-swapped cyt c_{552} oligomers were formed in *E. coli*, owing to the stability of the transient oligomer containing the apo protein before heme attachment. This is an indication that exceedingly stable proteins may have

disadvantages forming domain-swapped oligomers in cells.

3-3. Effect of domain-swapped oligomers on cell membranes

Cyt *c* exists in the inter-membranous space of mitochondria, and its release to the cytosol initiates apoptosis [37,38]. In cyt *c*, the side chains of many lysine residues are exposed to the solvent, and the positive charges of the lysine residues are involved in the interaction with the anionic CL in the mitochondria cell membrane, where the interaction plays a crucial role in triggering apoptosis by mediating release of cyt *c* to the cytosol [52]. It has been reported that cyt *c* induces spontaneous negative curvature at the CL-containing membrane, which can form lipid pores at the membrane surface [81]. When cyt *c* binds strongly to CL-rich domains, the CL-rich domains start to form small buds and eventually fold up into a collapsed state [82]. We found that anionic lipid domains were formed in the vesicles when the cyt *c* domain-swapped oligomers were added to the vesicles composed of anionic and neutral lipids (Figure 4) [83]. The number of lipid domains increased and the vesicle shrank over time, whereas no change occurred in the vesicle shapes following the addition of cyt *c* monomers. The positively charged area in the molecular surface of cyt *c* spread by the domain swapping oligomerization, and the electrostatic interaction with the negatively charged membrane surface increased for cyt *c* oligomers compared to the monomers, causing different effects on the vesicles. For the interaction with HeLa cells, many cells contracted and released from the culture dish when cyt *c* oligomers were added to the cells, whereas no significant change was observed in the cells when cyt *c* monomers were added (Figure 4). The membrane structures of HeLa cells were destroyed more by domain-swapped oligomers compared to monomers, due to the stronger interaction with the anionic lipids in the membrane surface for the oligomers. These results demonstrated that domain-swapped oligomers may exhibit different physiological functions

and cytotoxicity from those of the monomers.

4. Designing oligomers utilizing domain swapping

4-1. Heterodimers with different active sites

Four salt bridges were identified at the interface of the protomers in the domain-swapped Mb dimer (Figure 5Aa) [70]. These bridges resulted from electrostatic interactions between positively and negatively charged residues, holding the Mb protomers together. To construct a Mb dimer with two different heme active sites, two Mb surface mutants were constructed by modifying the charges of the residues at the salt bridge of the domain-swapped dimer; two positively charged residues were replaced with two negatively charged residues in one mutant, whereas two negatively charged residues were replaced with two positively charged residues in the other mutant (Figure 5Ab). Additionally, the heme site of one of the two Mb mutants was modified so that when it domain swapped with the other unmodified mutant through the introduced salt bridges, it resulted in the formation of a stable heterodimer with bis-His and His/H_2O active sites (PDB ID: 3WYO) [84]. The two sites in the domain-swapped heterodimer exhibited different reactivities upon reduction with the mild agent, ascorbic acid; the His/H_2O coordinate heme was reduced, while the bis-His site remained oxidized. Reduction of the Mb heterodimer with dithionite or ascorbic acid and subsequent exposure to air resulted in the formation of a heterodimer that contained an oxy heme and a ferric bis-His-coordinated heme.

PA cyt c_{551} and HT cyt c_{552} exhibit similar three-dimensional monomeric structures and their domain-swapped dimers exchange the N-terminal regions containing the N-terminal α-helix and heme between protomers, where the hinge loop locations are essentially the same (Figures 2A and 2B). To construct a *c*-type cyt heterodimer similar to what was performed with Mb, we constructed two chimeric proteins (PA cyt c_{551}–HT cyt c_{552} and HT cyt c_{552}–PA cyt c_{551}), in

which the sequences of N-terminal domain swapping regions were exchanged between the original proteins (Figure 5C) [85]. The two chimeric proteins formed a domain-swapped heterodimer with two His/Met coordinate hemes (PDB ID: 5XEC). The heme coordination structure of one of the two chimeric proteins was mutated to form a His/H_2O coordinate heme, and eventually a domain-swapped heterodimer with His/Met and His/H_2O coordinate hemes was obtained (PDB ID: 5XED; Figure 5D). The Fe−O_2 stretching band was observed at 580 cm^{-1} (554 cm^{-1} for its $^{18}O_2$ adduct) in the resonance Raman spectrum of the reduced/oxygenated heterodimer, which confirmed the binding of an oxygen molecule to its His/H_2O site. These results on the Mb heterodimer and *c*-type cyt heterodimer demonstrate that domain swapping is useful in designing multi-heme proteins with different active sites by modifying the protomer–protomer interaction and the active site in the domain-swapped dimer.

4-2. Domain swapping and unique structural oligomers

Unique structural heme protein oligomers have been constructed utilizing domain swapping. For example, the four-helix bundle protein cyt *cb*$_{562}$ formed a domain-swapped dimer (PDB ID: 5AWI; Figures 6A and B) [86]. The two helices in the N-terminal region of one protomer interacted with the other two helices in the C-terminal region of the other protomer in the cyt *cb*$_{562}$ dimer, except for the Lys51–Asp54 hinge loop, and the His/Met heme coordination structure of the dimer was similar to that of the monomer. Additionally, three domain-swapped cyt *cb*$_{562}$ dimers formed a unique nanocage with a Zn-SO_4 cluster inside the cavity in the crystal (Figures 6C and 6D). The Zn-SO_4 cluster consisted of fifteen Zn^{2+} and seven SO_4^{2-} ions, with the cage structure stabilized by coordination of the amino acid side chains of the dimers to the Zn^{2+} ions and connection of the two four-helix bundle units through a conformation-adjustable hinge loop.

To obtain more complex oligomeric structures, a building block protein (BBP) was constructed by circular permutation of the hyperthermostable AA cyt c_{555}. The angle of the intermolecular interactions of BBP molecules was controlled by cleaving the domain-swapping hinge loop of AA cyt c_{555} and connecting the original N- and C-terminal α-helices with an α-helical linker (Figure 7). BBP was expressed as a monomer in *E. coli*, whereas it formed oligomers up to ~40 mers with a relatively large amount of trimers when refolded under high protein concentration. BBP molecules domain swapped in the trimer, with the N-terminal region of one BBP molecule interacting intermolecularly with the C-terminal region of another BBP molecule, resulting in a triangle-shaped structure with an edge length of 68 Å (PDB ID: 5Z25; Figure 7) [87]. Additionally, four trimers assembled into a unique tetrahedron in the crystal. These results demonstrated that the circular permutation connecting the original N- and C-terminal α-helices with an α-helical linker enhances domain swapping considerably, and this method is useful for constructing organized protein structures.

Protein oligomer formation has also been controlled by utilizing domain swapping for a dimer–monomer transition protein, *Allochromatium vinosum* (AV) cyt *c′*. AV cyt *c′* is a homo-dimeric protein in its native form, in which its protomer exhibits a four-helix bundle structure containing a covalently bound five-coordinate heme as a gas binding site [88]. AV cyt *c′* exhibits a unique reversible dimer–monomer transition according to the absence and presence of CO. The sixth coordination site of AV cyt *c′* is occupied with the side chain of Tyr16, which has been suggested to be a trigger for the dimer-to-monomer transition upon CO binding to the heme [89]. AV cyt *c′* formed a domain-swapped dimer, and the dimer was utilized to form a tetramer, comprising one domain-swapped dimer subunit and two monomer subunits (PDB ID: 5GYR; Figure 8A) [90]. The heme environments of the monomer and domain-swapped dimer subunits of the tetramer were similar to those of the native dimer (Figure 8B). Interestingly,

oligomers were formed in the solution mainly containing domain-swapped dimers of AV cyt *c′* and dissociated to domain-swapped dimers by the addition of CO (Figure 8C). This is an example of utilizing domain swapping to construct and control a well-organized oligomeric structure.

Domain swapping has also been observed in amyloidogenic proteins, such as cystatins—a superfamily of structurally homologous cysteine proteinase inhibitors [45,91]. It has been reported that domain swapping tends to accelerate aggregation of proteins into amyloid-like fibrils [45,66,92,93]. The domain-swapped cyt *c* dimer formed a spherical assembly of amyloid fibrils by laser trapping, a method in which molecules are concentrated at the focal point, although amyloid fibrils were difficult to form by laser trapping of the cyt *c* monomer [94]. It was possible to manipulate spherical assemblies individually in solution to fabricate a three-dimensional micro-structure and a line pattern. These results demonstrated that domain-swapped oligomers can be used to obtain amyloid fibrils; thus, domain swapping may be applicable for investigating biological processes, such as amyloid fibril formation, with the combination of other analytical techniques.

5. Conclusion

According to Anfinsen's dogma, proteins have a specific three-dimensional structure corresponding to the primary sequence of amino acids. However, when domain swapping occurs, proteins that originally exist as monomers may form oligomers. This aspect implies that the structure of the protein determined by the amino acid sequence is not unique and encompasses diversity. In particular, heme proteins form oligomers by domain swapping relatively easily. The heme is hydrophobic and the hydrophobic interaction plays a major roll at the early stage of protein folding; thus, domain swapping may occur in many heme proteins,

due to the intermolecular hydrophobic interaction at the early stage of protein folding. It is surprising that oligomerization of heme proteins by domain swapping has not been widely recognized until recently, although protein structures and functions have been thoroughly studied for more than a hundred years. The research on domain swapping *in vivo*, as well as *in vitro*, is expected to develop more in the future, allowing us to understand the mechanism and properties of domain swapping and use it to construct new structural and functional heme protein oligomers.

Table of Abbreviations

AA, *Aquifex aeolicus*; AV, *Allochromatium vinosum*; BBP, building block protein; CL, cardiolipin; cyt, cytochrome; *E. coli*, *Escherichia coli*; ΔH, enthalpy change; HT, *Hydrogenobacter thermophilus*; Mb, myoglobin; PA, *Pseudomonas aeruginosa*; RNase, ribonuclease; WT, wild-type.

Acknowledgments

I deeply thank Dr. Satoshi Nagao, Dr. Masaru Yamanaka, Prof. Yoshiki Higuchi, and all the other coworkers involved in the works presented in this review. I am thankful to Mr. Leigh McDowell, Nara Institute of Science and Technology, for his advice on manuscript preparation. This work was partially supported by Grants-in-Aid for Scientific Research (Category B, No. JP18H02088, S.H.; Innovative Areas, No. JP18K19146, S.H.) from JSPS.

References

[1] H. Li, M. Eddaoudi, M. O'Keeffe, O.M. Yaghi, Nature 402 (1999) 276–279.

[2] S. Horike, S. Shimomura, S. Kitagawa, Nat. Chem. 1 (2009) 695–704.

[3] J. Lee, O.K. Farha, J. Roberts, K.A. Scheidt, S.T. Nguyen, J.T. Hupp, Chem. Soc. Rev. 38 (2009) 1450–1459.

[4] Y. Inokuma, M. Kawano, M. Fujita, Nat. Chem. 3 (2011) 349–358.

[5] L.E. Kreno, K. Leong, O.K. Farha, M. Allendorf, R.P. Van Duyne, J.T. Hupp, Chem. Rev. 112 (2012) 1105–1125.

[6] A. Messerschmidt, R. Huber, T. Poulos, T. Wieghardt (Eds.), Handbook of Metalloproteins, vol. 1, Wiley, New York, 2001.

[7] T.L. Poulos, Chem. Rev. 114 (2014) 3919–3962.

[8] K.D. Bewley, K.E. Ellis, M.A. Firer-Sherwood, S.J. Elliott, Biochim. Biophys. Acta 1827 (2013) 938–948.

[9] G.W. Chong, A.A. Karbelkar, M.Y. El-Naggar, Curr. Opin. Chem. Biol. 47 (2018) 7–17.

[10] J. Blumberger, Curr. Opin. Chem. Biol. 47 (2018) 24–31.

[11] E.N. Salgado, J. Faraone-Mennella, F.A. Tezcan, J. Am. Chem. Soc. 129 (2007) 13374–13375.

[12] J.D. Brodin, X.I. Ambroggio, C. Tang, K.N. Parent, T.S. Baker, F.A. Tezcan, Nat. Chem. 4 (2012) 375–382.

[13] K. Oohora, A. Onoda, T. Hayashi, Chem. Commun. 48 (2012) 11714–11726.

[14] K. Oohora, N. Fujimaki, R. Kajihara, H. Watanabe, T. Uchihashi, T. Hayashi, J. Am. Chem. Soc. 140 (2018) 10145–10148.

[15] M.J. Boerakker, J.M. Hannink, P.H. Bomans, P.M. Frederik, R.J. Nolte, E.M. Meijer, N.A. Sommerdijk, Angew. Chem. Int. Ed. 41 (2002) 4239–4241.

[16] A.J. Baldwin, R. Bader, J. Christodoulou, C.E. MacPhee, C.M. Dobson, P.D. Barker, J. Am. Chem. Soc. 128 (2006) 2162–2163.

[17] M. Fandrich, M.A. Fletcher, C.M. Dobson, Nature 410 (2001) 165–166.

[18] N.S. de Groot, S. Ventura, Spectroscopy 19 (2005) 199–205.

[19] M.J. Bennett, M.P. Schlunegger, D. Eisenberg, Protein Sci. 4 (1995) 2455-2468.

[20] Y. Liu, D. Eisenberg, Protein Sci. 11 (2002) 1285–1299.

[21] A.M. Gronenborn, Curr. Opin. Struct. Biol. 19 (2009) 39–49.

[22] F. Rousseau, J. Schymkowitz, L.S. Itzhaki, Adv. Exp. Med. Biol. 747 (2012) 137–152.

[23] A.M. Crestfield, W.H. Stein, S. Moore, Arch. Biochem. Biophys. Suppl 1 (1962) 217–222.

[24] M.J. Bennett, S. Choe, D. Eisenberg, Proc. Natl. Acad. Sci. USA 91 (1994) 3127–3131.

[25] M.A. Baker, R.M. Hynson, L.A. Ganuelas, N.S. Mohammadi, C.W. Liew, A.A. Rey, A.P. Duff, A.E. Whitten, C.M. Jeffries, N.J. Delalez, Y.V. Morimoto, D. Stock, J.P. Armitage, A.J. Turberfield, K. Namba, R.M. Berry, L.K. Lee, Nat. Struct. Mol. Biol. 23 (2016) 197–203.

[26] J.M. Reis, D.C. Burns, G.A. Woolley, Biochemistry 53 (2014) 5008–5016.

[27] J.M. Karchin, J.H. Ha, K.E. Namitz, M.S. Cosgrove, S.N. Loh, Sci. Rep. 7 (2017) 44388.

[28] R. Arai, N. Kobayashi, A. Kimura, T. Sato, K. Matsuo, A.F. Wang, J.M. Platt, L.H. Bradley, M.H. Hecht, J. Phys. Chem. B 116 (2012) 6789–6797.

[29] N. Kobayashi, K. Yanase, T. Sato, S. Unzai, M.H. Hecht, R. Arai, J. Am. Chem. Soc. 137 (2015) 11285–11293.

[30] D. Nurizzo, M.C. Silvestrini, M. Mathieu, F. Cutruzzolà, D. Bourgeois, V. Fülöp, J. Hajdu, M. Brunori, M. Tegoni, C. Cambillau, Structure 5 (1997) 1157–1171.

[31] B.R. Crane, R.J. Rosenfeld, A.S. Arvai, D.K. Ghosh, S. Ghosh, J.A. Tainer, D.J. Stuehr, E.D. Getzoff, EMBO J. 18 (1999) 6271–6281.

[32] G. Kurisu, H. Zhang, J.L. Smith, W.A. Cramer, Science 302 (2003) 1009–1014.

[33] M. Czjzek, S. Létoffé, C. Wandersman, M. Delepierre, A. Lecroisey, N. Izadi-Pruneyre, J. Mol. Biol. 365 (2007) 1176–1186.

[34] M.A. Silva, T.G. Lucas, C.A. Salgueiro, C.M. Gomes, PLoS One 7 (2012) e46328.

[35] K. Oohora, T. Hayashi, Curr. Opin. Chem. Biol. 19 (2014) 154–161.

[36] S. Hirota, Y.W. Lin, J. Biol. Inorg. Chem. 23 (2018) 7–25.

[37] P. Li, D. Nijhawan, I. Budihardjo, S.M. Srinivasula, M. Ahmad, E.S. Alnemri, X. Wang, Cell 91 (1997) 479–489.

[38] D. Spierings, G. McStay, M. Saleh, C. Bender, J. Chipuk, U. Maurer, D.R. Green, Science 310 (2005) 66–67.

[39] G.W. Bushnell, G.V. Louie, G.D. Brayer, J. Mol. Biol. 214 (1990) 585–595.

[40] R.E. Dickerson, T. Takano, D. Eisenberg, O.B. Kallai, L. Samson, A. Cooper, E. Margoliash, J. Biol. Chem. 246 (1971) 1511–1535.

[41] E. Margoliash, J. Lustgarten, J. Biol. Chem. 237 (1962) 3397–3405.

[42] S. Hirota, Y. Hattori, S. Nagao, M. Taketa, H. Komori, H. Kamikubo, Z. Wang, I. Takahashi, S. Negi, Y. Sugiura, M. Kataoka, Y. Higuchi, Proc. Natl. Acad. Sci. USA 107 (2010) 12854–12859.

[43] S. Sambashivan, Y. Liu, M.R. Sawaya, M. Gingery, D. Eisenberg, Nature 437 (2005) 266–269.

[44] M. Yamasaki, T.J. Sendall, M.C. Pearce, J.C. Whisstock, J.A. Huntington, EMBO Rep. 12 (2011) 1011–1017.

[45] M. Wahlbom, X. Wang, V. Lindstrom, E. Carlemalm, M. Jaskolski, A. Grubb, J. Biol. Chem. 282 (2007) 18318–18326.

[46] Z. Guo, D. Eisenberg, Proc. Natl. Acad. Sci. USA 103 (2006) 8042–8047.

[47] C. Liu, M.R. Sawaya, D. Eisenberg, Nat. Struct. Mol. Biol. 18 (2011) 49–55.

[48] P. Das, J.A. King, R. Zhou, Proc. Natl. Acad. Sci. USA 108 (2011) 10514–10519.

[49] A.D. Nugraheni, S. Nagao, S. Yanagisawa, T. Ogura, S. Hirota, J. Biol. Inorg. Chem. 18 (2013) 383–390.

[50] Z. Wang, T. Matsuo, S. Nagao, S. Hirota, Org. Biomol. Chem. 9 (2011) 4766–4769.

[51] L.J. McClelland, H.B.B. Steele, F.G. Whitby, T.C. Mou, D. Holley, J.B.A. Ross, S.R. Sprang, B.E. Bowler, J. Am. Chem. Soc. 138 (2016) 16770–16778.

[52] V.E. Kagan, V.A. Tyurin, J. Jiang, Y.Y. Tyurina, V.B. Ritov, A.A. Amoscato, A.N. Osipov, N.A. Belikova, A.A. Kapralov, V. Kini, Vlasova, II, Q. Zhao, M. Zou, P. Di, D.A. Svistunenko, I.V. Kurnikov, G.G. Borisenko, Nat. Chem. Biol. 1 (2005) 223–232.

[53] V.E. Kagan, G.G. Borisenko, Y.Y. Tyurina, V.A. Tyurin, J. Jiang, A.I. Potapovich, V. Kini, A.A. Amoscato, Y. Fujii, Free Radic. Biol. Med. 37 (2004) 1963–1985.

[54] M. Ott, J.D. Robertson, V. Gogvadze, B. Zhivotovsky, S. Orrenius, Proc. Natl. Acad. Sci. USA 99 (2002) 1259–1263.

[55] P. George, S.C. Glauser, A. Schejter, J. Biol. Chem. 242 (1967) 1690–1695.

[56] N. Yoshida, M. Higashi, H. Motoki, S. Hirota, J. Chem. Phys. 148 (2018) 025102.

[57] S. Hirota, N. Yamashiro, Z. Wang, S. Nagao, J. Biol. Inorg. Chem. 22 (2017) 705–712.

[58] Y. Hayashi, S. Nagao, H. Osuka, H. Komori, Y. Higuchi, S. Hirota, Biochemistry 51 (2012) 8608–8616.

[59] Y. Matsuura, T. Takano, R.E. Dickerson, J. Mol. Biol. 156 (1982) 389–409.

[60] C. Travaglini-Allocatelli, S. Gianni, V.K. Dubey, A. Borgia, A. Di Matteo, D. Bonivento, F. Cutruzzolà, K.L. Bren, M. Brunori, J. Biol. Chem. 280 (2005) 25729–25734.

[61] S. Nagao, M. Ueda, H. Osuka, H. Komori, H. Kamikubo, M. Kataoka, Y. Higuchi, S. Hirota, PLoS One 10 (2015) e0123653.

[62] C. Ren, S. Nagao, M. Yamanaka, H. Komori, Y. Shomura, Y. Higuchi, S. Hirota, Mol. Biosyst. 11 (2015) 3218–3221.

[63] Y. Liu, P.J. Hart, M.P. Schlunegger, D. Eisenberg, Proc. Natl. Acad. Sci. USA 95 (1998) 3437–3442.

[64] Y. Liu, G. Gotte, M. Libonati, D. Eisenberg, Nat. Struct. Biol. 8 (2001) 211–214.

[65] G. Gotte, A. Mahmoud Helmy, C. Ercole, R. Spadaccini, D.V. Laurents, M. Donadelli, D. Picone, PLoS One 7 (2012) e46804.

[66] M. Orlikowska, E. Jankowska, R. Kołodziejczyk, M. Jaskólski, A. Szymańska, J. Struct. Biol. 173 (2011) 406–413.

[67] N. Nandwani, P. Surana, J.B. Udgaonkar, R. Das, S. Gosavi, Protein Sci. 26 (2017) 1994–2002.

[68] M. Obuchi, K. Kawahara, D. Motooka, S. Nakamura, M. Yamanaka, T. Takeda, S. Uchiyama, Y. Kobayashi, T. Ohkubo, Y. Sambongi, Acta Crystallogr. D Biol. Crystallogr. 65 (2009) 804–813.

[69] M. Yamanaka, S. Nagao, H. Komori, Y. Higuchi, S. Hirota, Protein Sci. 24 (2015) 366–375.

[70] S. Nagao, H. Osuka, T. Yamada, T. Uni, Y. Shomura, K. Imai, Y. Higuchi, S. Hirota, Dalton Trans. 41 (2012) 11378–11385.

[71] S. Nagao, H. Ishikawa, T. Yamada, Y. Mizutani, S. Hirota, J. Biol. Inorg. Chem. 20 (2015) 523–530.

[72] C. Savino, A.E. Miele, F. Draghi, K.A. Johnson, G. Sciara, M. Brunori, B. Vallone, Biopolymers 91 (2009) 1097–1107.

[73] S. Hirota, M. Ueda, Y. Hayashi, S. Nagao, H. Kamikubo, M. Kataoka, J. Biochem. 152 (2012) 521–529.

[74] P.P. Parui, M.S. Deshpande, S. Nagao, H. Kamikubo, H. Komori, Y. Higuchi, M. Kataoka, S. Hirota, Biochemistry 52 (2013) 8732–8744.

[75] H. Roder, G.A. Elove, S.W. Englander, Nature 335 (1988) 700–704.

[76] W.B. Hu, Z.Y. Kan, L. Mayne, S.W. Englander, Proc. Natl. Acad. Sci. USA 113 (2016) 3809–3814.

[77] J.P. López-Alonso, M. Bruix, J. Font, M. Ribó, M. Vilanova, M.A. Jiménez, J. Santoro, C. González, D.V. Laurents, J. Am. Chem. Soc. 132 (2010) 1621–1630.

[78] M.S. Deshpande, P.P. Parui, H. Kamikubo, M. Yamanaka, S. Nagao, H. Komori, M. Kataoka, Y. Higuchi, S. Hirota, Biochemistry 53 (2014) 4696–4703.

[79] K. Ono, M. Ito, S. Hirota, S. Takada, Phys. Chem. Chem. Phys. 17 (2015) 5006–5013.

[80] Y. Hayashi, M. Yamanaka, S. Nagao, H. Komori, Y. Higuchi, S. Hirota, Sci. Rep. 6 (2016) 19334.

[81] C.L. Bergstrom, P.A. Beales, Y. Lv, T.K. Vanderlick, J.T. Groves, Proc. Natl. Acad. Sci. USA 110 (2013) 6269-6274.

[82] P.A. Beales, C.L. Bergstrom, N. Geerts, J.T. Groves, T.K. Vanderlick, Langmuir 27 (2011) 6107–6115.

[83] S. Junedi, K. Yasuhara, S. Nagao, J. Kikuchi, S. Hirota, Chembiochem 15 (2014) 517–521.

[84] Y.-W. Lin, S. Nagao, M. Zhang, Y. Shomura, Y. Higuchi, S. Hirota, Angew. Chem. Int. Ed. 54 (2015) 511–515.

[85] M. Zhang, T. Nakanishi, M. Yamanaka, S. Nagao, S. Yanagisawa, Y. Shomura, N. Shibata, T. Ogura, Y. Higuchi, S. Hirota, Chembiochem 18 (2017) 1712–1715.

[86] T. Miyamoto, M. Kuribayashi, S. Nagao, Y. Shomura, Y. Higuchi, S. Hirota, Chem. Sci. 6 (2015) 7336–7342.

[87] A. Oda, S. Nagao, M. Yamanaka, I. Ueda, H. Watanabe, T. Uchihashi, N. Shibata, Y. Higuchi, S. Hirota, Chem. Asian J. 13 (2018) 964–967.

[88] M.A. Hough, C.R. Andrew, Adv. Microb. Physiol. 67 (2015) 1–84.

[89] Z. Ren, T. Meyer, D.E. McRee, J. Mol. Biol. 234 (1993) 433–445.

[90] M. Yamanaka, M. Hoshizumi, S. Nagao, R. Nakayama, N. Shibata, Y. Higuchi, S. Hirota, Protein Sci. 26 (2017) 464–474.

[91] A. Sanders, C.J. Craven, L.D. Higgins, S. Giannini, M.J. Conroy, A.M. Hounslow, J.P. Waltho, R.A. Staniforth, J. Mol. Biol. 336 (2004) 165–178.

[92] J.M. Louis, I.J. Byeon, U. Baxa, A.M. Gronenborn, J. Mol. Biol. 348 (2005) 687–698.

[93] A. Taler-Verčič, S. Hasanbašić, S. Berbić, V. Stoka, D. Turk, E. Žerovnik, Int. J. Mol. Sci. 18 (2017) 549.

[94] K.I. Yuyama, M. Ueda, S. Nagao, S. Hirota, T. Sugiyama, H. Masuhara, Angew. Chem. Int. Ed. 56 (2017) 6739–6743.

Table 1

Examples of domain-swapped heme proteins.

Protein	type of oligomer	PDB ID	swapping region	hinge region	heme coordination	high-order structure	reference
horse cyt *c*	dimer	3NBS	C-terminal α-helix	Thr78–Ala83	His/H_2O	–	[42]
horse cyt *c*	trimer	3NBT	C-terminal α-helix	Thr79–Ala83	His/H_2O	–	[42]
yeast iso-1-cyt *c* (with detergent)	dimer	5KKE (5T7H, 5KLU)	C-terminal α-helix	Asn70–Gly84	His/Met	–	[51]
PA cyt c_{551}	dimer	3X39	N-terminal α-helix and heme	Thr20–Met22	His/Met	–	[61]
HT cyt c_{552}	dimer	3VYM	N-terminal α-helix and heme	Ala18–Lys20	His/Met	–	[58]
HT cyt c_{552} insG3 mutant	major dimer	5AUR	N-terminal α-helix and heme	Ala18–Lys23	His/Met	–	[62]
HT cyt c_{552} insG3 mutant	minor dimer	5AUS	C-terminal α-helix	Trp57–Ser59	His/Met	–	[62]
AA cyt c_{555}	dimer	3X15	C-terminal α-helix and extra 3_{10}-α-3_{10} helix	Val53–Lys57	His/Met	tetramer (one domain-swapped dimer and two monomers)	[69]
cyt cb_{562}	dimer	5AWI	two α-helices	Lys51–Asp54	His/Met	cage (three domain-swapped dimers)	[86]
AV cyt *c*′	dimer	5GYR	two α-helices	Glu79–Gly85	His (5-coordinate)	–	[90]
PA cyt cd_1 nitrite reductase	dimer	1NIR	N-terminal arm	–	His/Met, His (5-coordinate)	–	[30]
murine iNOS	dimer	1DF1	N-terminal β-hairpin	Cys104–Lys107	Cys (5-coordinate)	–	[31]
Serratia marcescens HasA	dimer	2CN4	N-terminal α-helix and arm	Gly43–Gly48	His/Tyr	–	[33]
Geobacter sulfurreducens	dimer	3B42	N-terminal and	–	His/Met	–	[34]

GSU0935 sensor domain			successive α-helices				
horse Mb	dimer	3VM9	globular	Lys78–Glu85	His/H_2O	–	[70]
c-type cyt	heterodimer	5XEC	N-terminal α-helix and heme	Thr20–Lys22, Ala18–Met20	His/His, His/His	–	[85]
c-type cyt	heterodimer	5XED	N-terminal α-helix and heme	Thr20–Lys22, Ala18–Met20	His/His, His/H_2O	–	[85]
Mb	heterodimer	3WYO	globular	Lys78–Glu85	His/His, His/H_2O	–	[84]
designed protein from AA cyt c_{555}	trimer	5Z25	N-terminal extra 3_{10}-α-3_{10} helix and α-helix	(inserted α-helix linker)	His/Met	tetrahedron (four domain-swapped trimers)	[87]

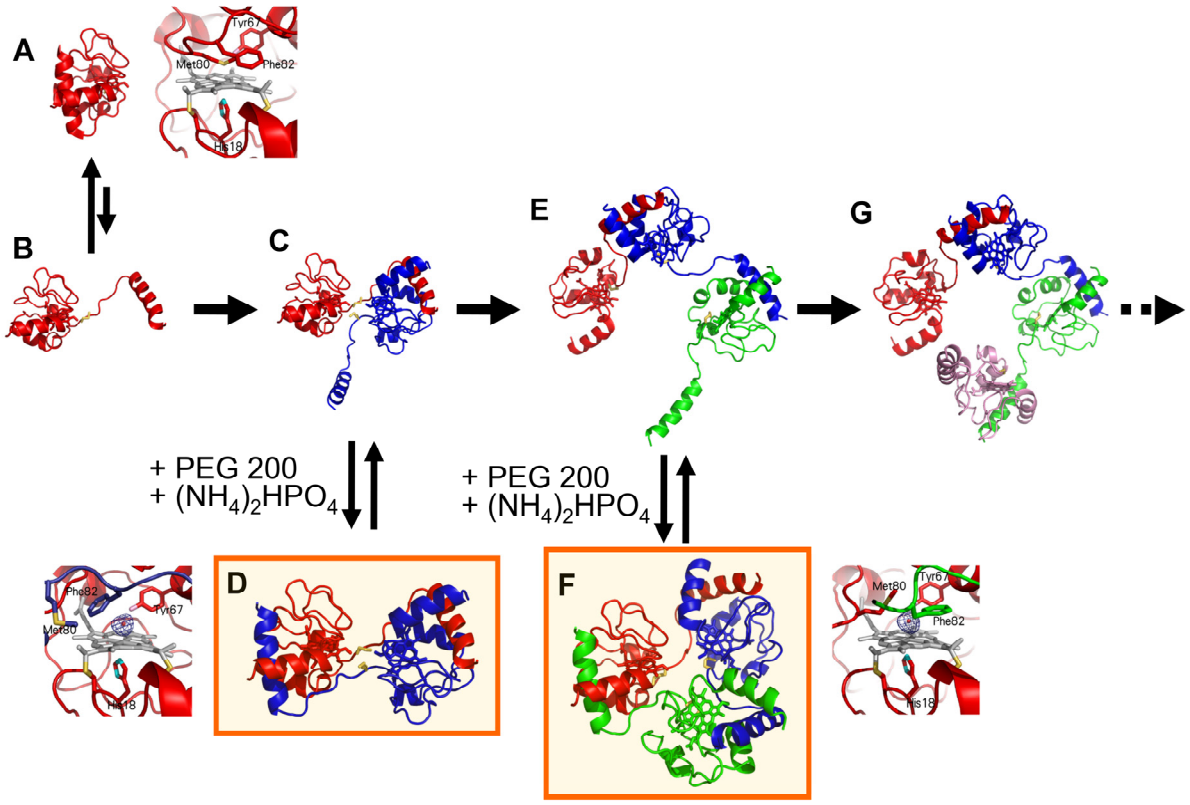

Fig. 1. Schematic view of cyt *c* polymerization. (A) Protein and active site structures of monomeric cyt *c* (PDB: 1HRC) [39]. (B) Model of monomeric cyt *c* in solution. (C) Model of dimeric cyt *c* in solution. (D) Protein and active site structures of dimeric cyt *c* (PDB: 3NBS) [42]. (E) Model of trimeric cyt *c* in solution. (F) Protein and active site structures of trimeric cyt *c* (PDB: 3NBT) [42]. (G) Model of tetrameric cyt *c* in solution. Met80 is highlighted in yellow. Adapted with permission from ref. [42]. Copyright 2010 National Academy of Sciences.

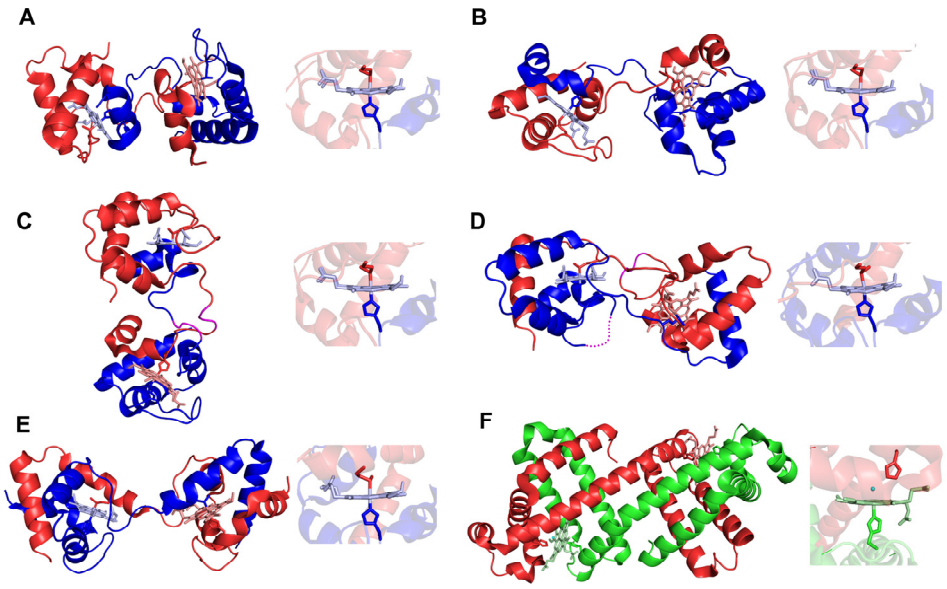

Fig. 2. Three-dimensional and active site structures of domain-swapped dimers of *c*-type cyts and Mb: (A) PA cyt c_{551} (PDB ID: 3X39), (B) HT cyt c_{552} (PDB ID: 3VYM), (C) HT cyt c_{552} insG3 mutant (major dimer, PDB ID: 5AUR), (D) HT cyt c_{552} insG3 mutant (minor dimer, PDB ID: 5AUS), (E) AA cyt c_{555} (PDB ID: 3X15), and (F) horse Mb (PDB ID: 3VM9).

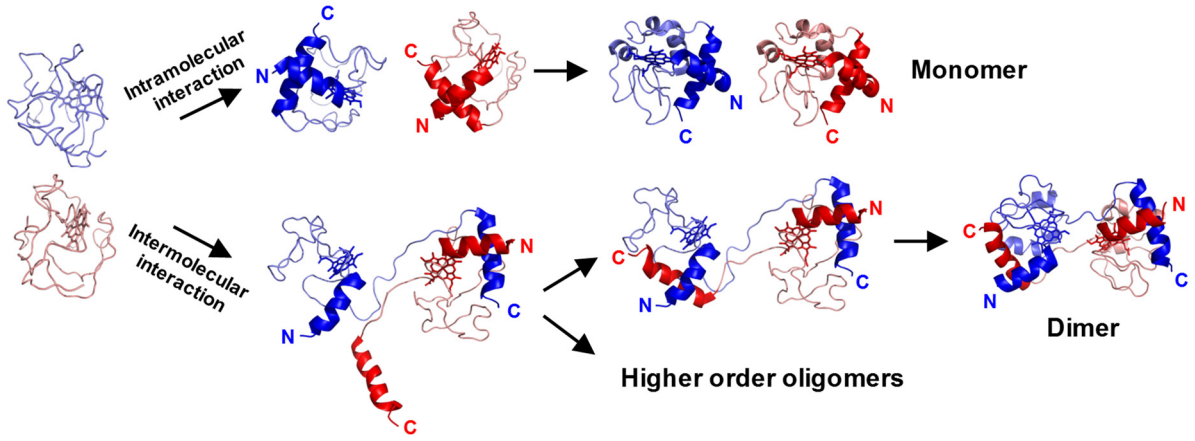

Fig. 3. Schematic view of cyt *c* oligomerization by protein folding. Cyt *c* oligomers are formed by intermolecular interactions during the folding process, whereas monomers are formed by intramolecular interactions. Adapted with permission from ref. [74]. Copyright 2013 American Chemical Society.

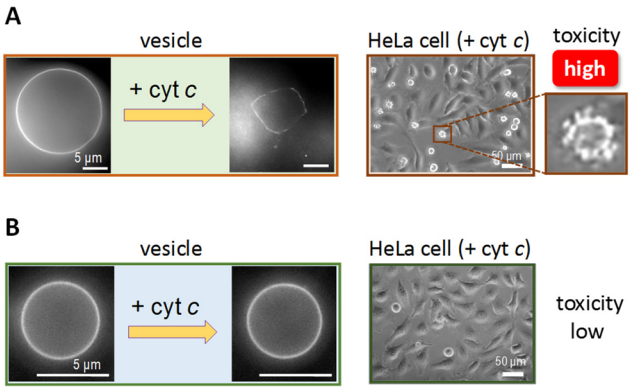

Fig. 4. Morphological changes in vesicles and cell membranes by interaction with (A) domain-swapped oligomers and (B) monomers of cyt *c*. Membrane destruction was observed when cyt *c* oligomers interacted with the membrane. Adapted with permission from ref. [83]. Copyright 2014 Wiley-VCH.

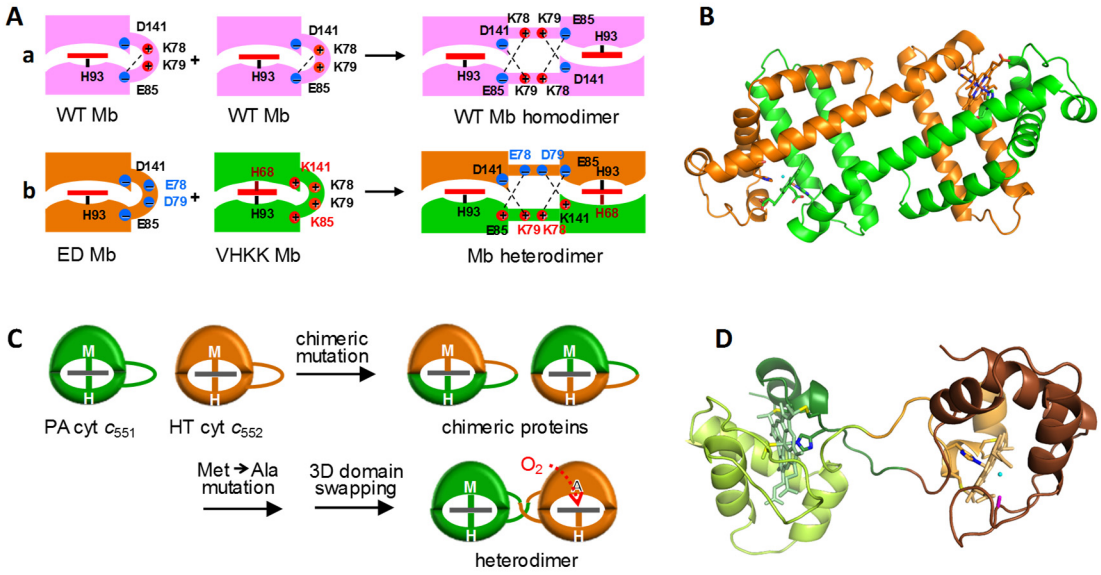

Fig. 5. Construction of heterodimers with different active sites based on domain swapping: (A) Design and (B) three-dimensional structure (PDB ID: 3WYO) of Mb heterodimer. Adapted with permission from ref. [84]. Copyright 2015 Wiley-VCH. (C) Design and (D) three-dimensional structure (PDB ID: 5XED) of *c*-type cyt heterodimer. Adapted with permission from ref. [85]. Copyright 2017 The Royal Society of Chemistry.

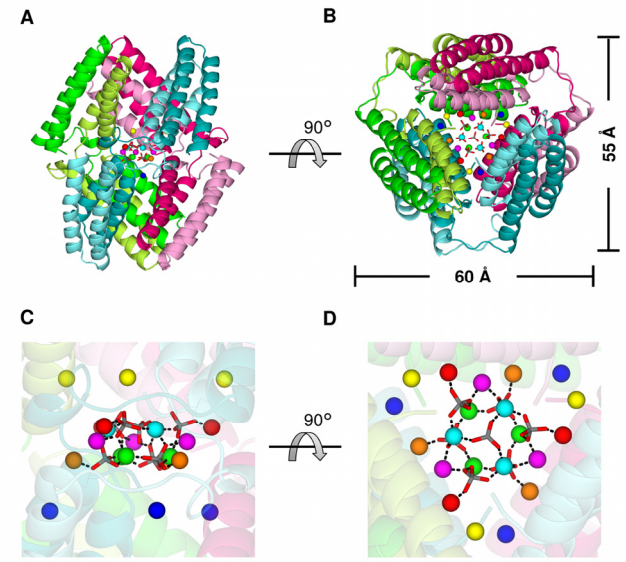

Fig. 6. Cage structure constructed of three domain-swapped cyt *cb*$_{562}$ dimers (PDB ID: 5AWI): (A, B) The overall structure of the cage. B is a 90°-rotated view of A. The three dimers forming the cage are shown in combinations of green and light-green, blue-green and cyan, and red and pink, respectively. (C, D) Enlarged views of the Zn^{2+} and SO_4^{2-} ions in the internal cavity. D is a 90°-rotated view of C. The coordination bonds between Zn^{2+} and SO_4^{2-} ions are shown as black dash lines. The Zn^{2+} ions are shown as green, cyan, magenta, orange, red, yellow, and blue spheres. The SO_4^{2-} ions are shown as stick models, and their sulfur and oxygen atoms are coloured grey and red, respectively. Adapted with permission from ref. [86]. Copyright 2015 The Royal Society of Chemistry.

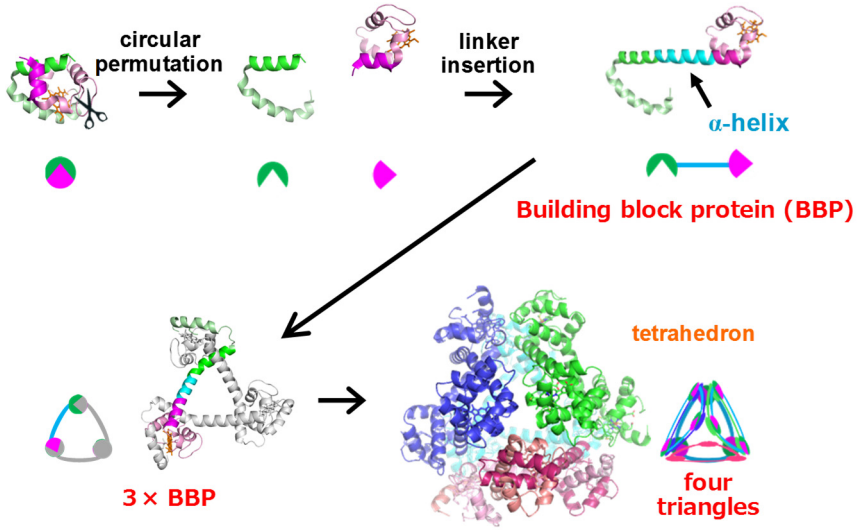

Fig. 7. Schematic representation of the BBP design and its trimer and tetrahedron formations (PDB ID: 5Z25). N- and C-terminal regions of AA cyt c_{555} are depicted in magenta and green, respectively. The hemes are shown as orange stick models in the protein structures.

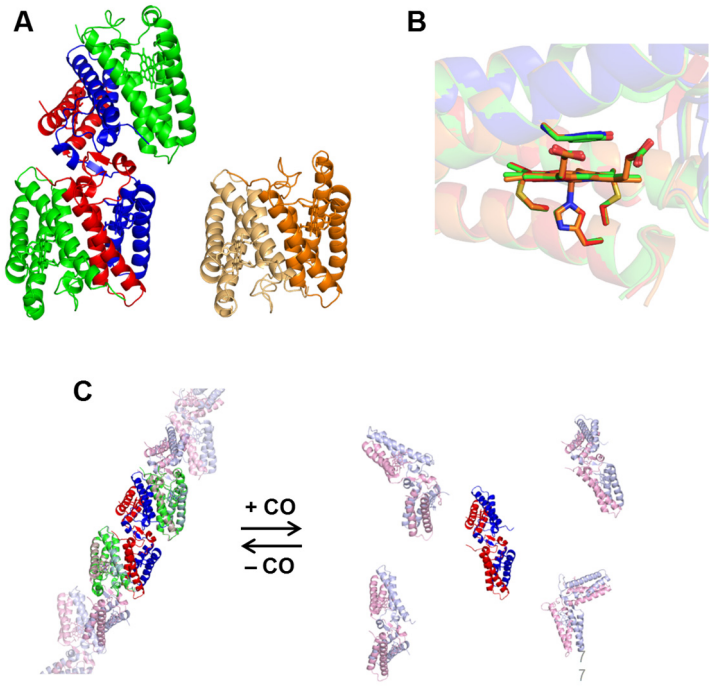

Fig. 8. (A) X-ray crystal structure of tetrameric AV cyt *c′* (PDB ID: 5GYR). Tetrameric AVCP comprised a domain-swapped dimer subunit (red and blue) and two monomer subunits (green). The structure of the AV cyt *c′* native dimer (orange, PDB ID: 1BBH) is also shown for comparison. (B) Superimposed figure of the active site structures of the AV cyt *c′* native dimer and domain-swapped dimer. The monomer and domain-swapped dimer subunits of the tetramer are depicted in green and red/blue, respectively. (C) Schematic view of the oligomer association and dissociation of domain-swapped AV cyt *c′* dimers controlled by binding of carbon monoxide to the heme of AV cyt *c′*. Adapted with permission from ref. [90]. Copyright 2017 Wiley.